

Chapter 5

Imaging the Cortical Representation of Active Sensing in the Vibrissa System

Fritjof Helmchen and Jerry L. Chen

Abstract Rodents explore the environment with their facial whiskers using active whisking to collect information about object location and identity. The sensory information gathered is processed in the vibrissa system, a hierarchical network of interacting brain regions, comprising brainstem nuclei, thalamus subdivisions and neocortical regions. In the neocortex, neural representations of whisking and touch are formed to guide and adapt behavior given the environmental context. The exact features of these representations and their spatiotemporal dynamics still remain elusive. In this chapter, we provide an overview of *in vivo* functional imaging techniques that enable the study of spatiotemporal profiles of cortical activity during whisking-based behavior. We discuss imaging applications covering the large scale as well as the level of local cellular circuits, with a special focus on studies employing two-photon calcium imaging. We summarize recent findings on the cortical representation of passive and active sensation and of task-relevant whisker dynamics.

Keywords Barrel cortex · Active whisking · Neocortical regions · Voltage imaging · Two-photon calcium imaging · Object localization · Texture discrimination

Introduction

For multiple reasons the rodent whisker system is a well suited model for studying tactile information processing in the mammalian brain. Touching objects or conspecifics with facial whiskers is a highly behaviorally relevant sensing modality for rats and mice [1]. Rodents intentionally move their whiskers in characteristic ways to touch and gather tactile information, an example *par excellence* of active sensing [2]. The processing of tactile stimuli is organized in neural pathways at all

F. Helmchen (✉) · J. L. Chen
Laboratory of Neural Circuit Dynamics, Brain Research Institute, University of Zurich,
Winterthurerstrasse 190, 8057 Zurich, Switzerland
e-mail: helmchen@hifo.uzh.ch

J. L. Chen
e-mail: jerry.chen@hifo.uzh.ch

© Springer Science+Business Media, LLC 2015
P. Krieger, A. Groh (eds.), *Sensorimotor Integration in the Whisker System*,
DOI 10.1007/978-1-4939-2975-7_5

key levels of mammalian somatosensory computation, including brainstem loops, relay pathways through thalamic nuclei, thalamocortical loops, and especially cortical representations that feed into descending pathways for behavior control [3, 4]. Further, the importance of tactile sensation is reflected in the disproportionately large representation of the whisker pad in the barrel field (BF) of the primary somatosensory area (S1), with a well-defined somatotopic layout. This clear anatomy has invited numerous studies of cortical signal flow, the underlying synaptic interactions, and neural circuit mechanisms related to whisker motion and touch, within S1 and beyond. Another advantageous feature of the whisker system is the ease with which whiskers can be mechanically stimulated in a controlled manner (or, alternatively, trimmed or plucked to deprive the brain from this sensory input). Such manipulations have been widely adopted to investigate mechanisms of neural plasticity [5–7]. Finally, rats and mice can be well trained in whisker-dependent tasks, enabling studies of the neural basis of learning, decision making and other high-level brain functions.

In this chapter we focus on the neocortical level of the whisker system. The S1 barrel field connects to multiple other cortical areas via cortico-cortical axonal projections. For example, a strong connecting pathway exists to the contralateral S1 via the corpus callosum. In addition, S1 connects ipsilaterally to the smaller, more laterally positioned secondary somatosensory area (S2) and to the more anterior, medial primary motor cortex region (M1) (Fig. 5.1a). The S1-S2-M1 triangle forms the core of cortical sensorimotor integration, tied together by reciprocal connections but also connecting to further cortical areas [8–11]. Because of the widespread connectivity pattern among cortical regions, it can be expected that signal processing does not occur in isolation in individual areas but rather is likely to be governed by the interplay of all these areas. For the topic of this chapter, we note that the key cortical areas are located on the dorsal surface of the mouse brain and thus are accessible for imaging, either by implanting chronic glass windows or by thinning the overlying skull. S1 and M1 thus presumably have come into the focus of imaging research not only because of their conceptual importance as primary cortical areas but also for this ease of access.

On the local-circuit level, six-layered barrel cortex has been dissected in considerable detail, yet our understanding of this microcircuit is still incomplete. Similar to other primary sensory areas of the neocortex, the major neuronal cell types in the BF have been characterized in terms of their morphologies and anatomical distributions, their intrinsic biophysical properties, and their synaptic connections with neighboring cells or cells in other layers [12–15]. Electrophysiological recordings have been particularly informative in this respect, including extensive studies in brain slice preparations [5, 16] and more recently intracellular recordings *in vivo*, in anesthetized animals and in head-restrained awake, behaving animals [17–20]. A special focus has been the investigation of the functional relevance of specific subtypes of GABAergic interneurons [21], including prominently the parvalbumin(PV)-positive interneurons [22], the somatostatin(SOM)-positive interneurons [23, 24] and the interneurons positive for the vasoactive intestinal polypeptide (VIP). The latter group is a subgroup of the larger, recently identified group of interneurons

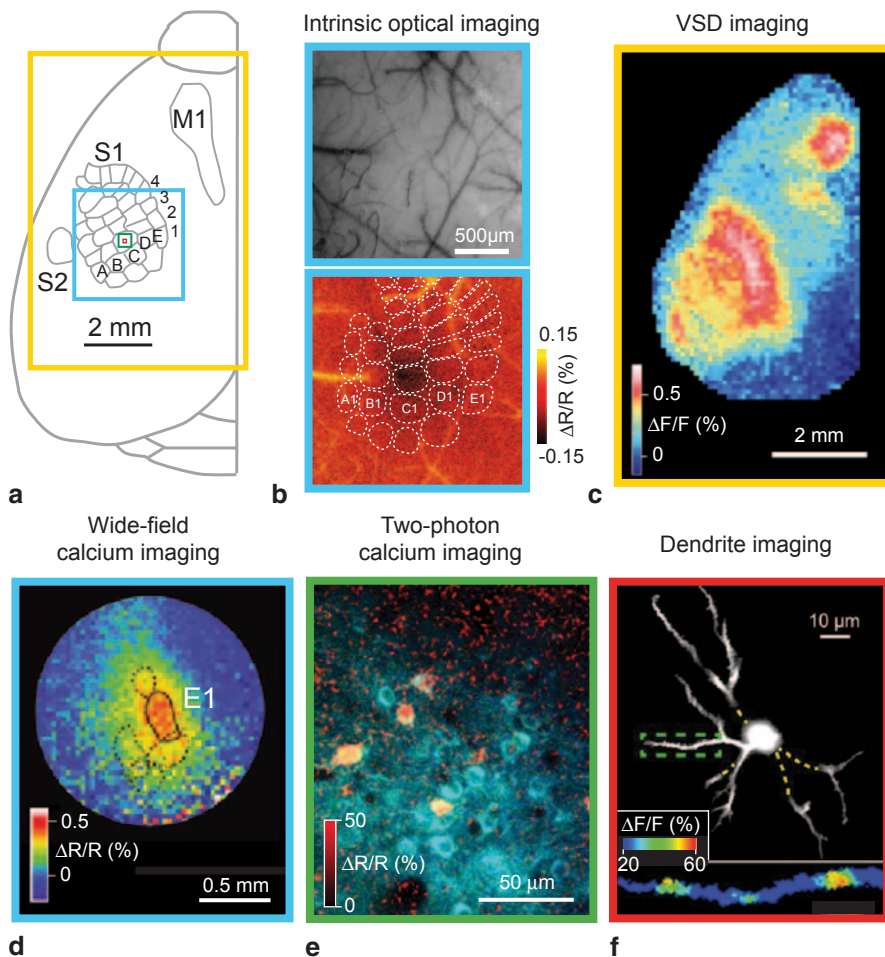


Fig. 5.1 Various imaging modalities to study barrel cortex function. **a** Overview of the different spatial scales covered by various imaging techniques, including hemisphere-wide field of views (yellow), barrel cortex imaging (blue), cellular imaging within a barrel column (green) and single-cell imaging (red). **b** Intrinsic optical imaging is performed by illuminating the cortical surface (top) with light (typically using 630-nm wavelength) and mapping the relative percentage changes in reflectance ($\Delta R/R$; bottom) upon whisker stimulation. Adapted from Petersen, 2007 [16]. **c** Wide-field VSD imaging. The example image was recorded in a urethane-anesthetized mouse with the voltage-sensitive dye RH1691 and shows the activity pattern 30 ms after a single-whisker stimulation, displaying the spread in S1 and a secondary activation spot in motor cortex (average of 10 trials; adapted from Ferezou et al. 2007 [36]). **d** Functional imaging across the barrel field can be performed by using wide-field calcium imaging with a camera. This example shows the onset activation map after stimulation of the E1 whisker, measured through a chronic cranial window with the ratiometric GECI YC3.60 following viral induction of indicator expression. $\Delta R/R$ indicates the changes in fluorescence ratio (mean of 20 trials). Adapted from Minderer et al. 2012 [58] with permission from John Wiley and Sons. **e** Two-photon calcium imaging of L2/3 neuronal activity in barrel cortex in an awake mouse performing a texture discrimination task. The image was acquired with the ratiometric indicator YCNano-140 and shows strong activation of a subset

expressing the ionotropic serotonin receptor 5HT_{3aR} [25]. VIP-positive interneurons have been functionally implicated in cortical disinhibition [26, 27].

While electrophysiological studies provided a wealth of functional data on neuronal activity in barrel cortex, and continue to do so, here we focus on the application of imaging techniques to study cortical dynamics in the whisker system. Imaging methods are complementary to electrophysiological methods in many ways and often these two activity measures can be combined in beneficial ways. Important advantages of imaging methods are that they enable (1) a large-scale view of cortical signal flow; (2) population recordings from identified neurons in relatively large networks of up to hundreds of neurons; and (3) functional measurements from subcellular structures such as axons, dendrites, and dendritic spines that are hardly accessible with electrophysiology. This chapter provides an overview of *in vivo* imaging approaches and highlights results that were obtained over the past decade for cortical dynamics in adult animals. We put special emphasis on imaging studies in awake, behaving animals, which have become feasible only recently.

Imaging Global and Local Cortical Representations of Whisker Dynamics

A variety of optical imaging methods can be applied to measure *in vivo* cortical activity evoked by active whisker movements or mechanical whisker stimulation. These methods cover distinct spatial scales, ranging from very local measurements at individual synaptic contacts to a global view of activity patterns across an entire hemisphere (Fig. 5.1a). They also differ with respect to their capability to resolve individual neurons and their temporal resolution for measuring subthreshold and/or suprathreshold activity. In the following we summarize the principles of the imaging techniques that are used to study the rodent vibrissa system.

Wide-Field Imaging of Intrinsic Signals

Large-scale imaging with sensitive CCD cameras has a long tradition in barrel cortex research, starting with optical imaging of intrinsic signals [28, 29]. The exposed cortical surface is illuminated with light (typically red light at around 630-nm wavelength) and the reflected light is imaged with a large field-of-view objective and a sensitive camera, capturing areas of several square millimeters. The degree of reflectance depends on the absorptive and scattering properties of the tissue, which change upon neuronal activation in part due to associated blood flow changes. Stimulation of a single whisker results in a localized, albeit blurry reflectance change, making it possible to determine where the barrel column is located that receives the

of neurons upon touching a presented texture with the whiskers. (Adapted From Chen et al. 2013b [80] with permission). **f** Calcium imaging of dendritic activity following single-neuron loading with Alexa Fluor 594 and the calcium indicator Oregon Green BAPTA-1. The Alexa-filled neuron with its dendrites is shown at the top. Localized $\Delta F/F$ changes in a selected dendrite following whisker stimulation are shown at the bottom. (Adapted from Varga et al. 2011 [84])

principal input from the stimulated whisker (Fig. 5.1b). Intrinsic signal changes are small ($<1\%$) and rather slow and therefore cannot resolve cortical dynamics with high temporal resolution. On the other hand, no dye-labeling is required and signal changes can be detected through the intact (thinned) skull. Because of its simplicity, intrinsic signal optical imaging has developed into a standard method for functional mapping of the barrel field *in vivo*, which is especially useful for targeting a specific barrel column [30]. In addition, imaging of intrinsic signal changes has contributed to studies of map plasticity, revealing expansion or shrinkage of single-whisker maps following sensory deprivation of surround whiskers and exposure to natural habitats, respectively [6, 31, 32]. More recently, map changes have been assessed in various transgenic mouse models of diseases [33, 34].

Wide-Field Fluorescence Imaging of Voltage Indicators

Whereas intrinsic signal imaging does not require previous dye labeling, staining cortical tissue with fluorescent indicators provides further opportunities to measure the spread of cortical activity related to whisker use. A direct visualization of electrical activity in neuronal populations is possible with voltage-sensitive dye (VSD) imaging, which is a classical experimental approach to measure cortical maps with high temporal resolution [35]. Various organic dyes have been developed that label cellular membranes and report membrane potential changes. For *in vivo* imaging, the cortical surface is soaked in a VSD-containing solution so that dye molecules penetrate the tissue and stain neuronal membranes. The measured fluorescence signal corresponds to the bulk average of the local membrane potential changes in the tissue (for cortical measurements originating mainly from supragranular layers) [18]. This method lacks cellular resolution but can reveal fast signal dynamics (up to kHz frequency range) with a sufficiently fast VSD and a high-speed camera.

VSD imaging of barrel cortex in the anesthetized rat revealed that following a single-whisker stimulation an initially highly localized cortical activity (at the location of the principal barrel column) rapidly spreads across the entire barrel field within 50 ms, with particularly high speed along the whisker row representation [18]. In follow-up studies on mouse neocortex, the field-of-view of VSD imaging was expanded to comprise nearly the entire dorsal surface of the neocortex, covering even both hemispheres [36, 37]. This global view uncovered that shortly after the S1 activation in the hemisphere contralateral to the single-whisker stimulus, another focal activation spot appears in the motor cortex, triggering a secondary wave of activity in frontal regions (Fig. 5.1c). In addition, S1 regions in the hemisphere ipsilateral to the stimulus are activated with a delay too. These examples demonstrate the brain-wide dimension of cortical processing, even following a simple brief stimulus, mediated via the dense cortico-cortical connections, here particularly from S1 to M1 [36, 38]. While high temporal resolution and direct read out of membrane potential changes are clear advantages of the VSD imaging technique, it is difficult to perform repeated measurements over long time periods using synthetic organic VSDs, which may also present potential pharmacological side effects [39].

The development and application of voltage-sensitive fluorescent proteins (VS-FPs) represents a highly promising alternative to organic dyes. Stable and long-

term expression of these genetically-encoded voltage indicators (GEVIs) can be achieved using either viral delivery or in transgenic mice (e.g., VSFP-Butterfly1.2, JAX® Mice, Stock Nr. 023528), potentially even targeting specific cellular subtypes. VSFPs have been applied, for example, to resolve whisker-evoked single-trial responses in the barrel cortex map [40, 41]. Further transgenic mouse lines have now become available [42]. Recently, new sensitive and fast VSFPs have been introduced, e.g., ‘Arch’ [43], ‘ArcLight’ [44], ‘MacQ’ [45], or ‘ASAP1’ [46]; *in vivo* applications of these new indicators are currently gaining momentum with great prospects of novel opportunities to chronically study fast cortex-wide signal flow patterns and oscillatory phenomena during behavior.

Wide-Field Fluorescence Imaging of Calcium Indicators

Besides fluorescent voltage indicators, the most prominent indicators of neuronal activity are calcium indicators. In fact, fluorescent calcium indicators still are the best characterized and most widely used indicators due to their large dynamic range and superior signal-to-noise ratio. In all neurons, the generation of an action potential is associated with the activation of voltage-gated calcium channels, causing a brief influx of calcium ions and thus allowing calcium indicators to serve as ‘action potential detectors’. The action-potential evoked change in intracellular calcium concentration is reported as a transient fluorescence change, typically lasting for a few hundred milliseconds in the cell soma [47, 48]. Calcium indicators furthermore can uncover localized calcium influx in dendrites, axons, and in pre- and postsynaptic structures, where calcium ions also exert important physiological functions as second messenger.

Since the introduction of the first genetically-encoded calcium indicator (GECI) ‘cameleon’ [49], the palette of available GECIs has largely expanded. Indicators have steadily become more sensitive, meanwhile outperforming the best traditional small-molecule indicators such as Oregon Green BAPTA-1. One class of GECIs is composed of a single fluorescent protein (FP) attached to a calcium-binding domain that triggers a conformational switch and thus translates calcium binding into a fluorescence change. A second class of GECIs consists of two FPs linked via a calcium-binding domain such that the distance and relative orientation between the FPs—and therefore the ‘fluorescence resonance energy transfer’ (FRET) between them—are modulated in a calcium concentration-dependent manner. By reading out the fluorescence signal emissions in two spectral windows, these indicators enable ratiometric measurements, which normalize for various factors including motion artifacts and can be calibrated in terms of absolute calcium concentrations. At present, the most popular GECIs are the newest single-FP GCaMP indicators [50, 51] and the best variants of ratiometric dual-FP GECIs, designed with a linker derived from either calmodulin [52, 53] or troponin [54, 55].

Following up on earlier work using the synthetic calcium indicator Oregon Green BAPTA-1 [56] GECIs are now employed for wide-field fluorescence imaging of cortical activity. A standard method to induce GECI expression is viral delivery, especially using adeno-associated virus (AAV) constructs with neuron-specific promoters [57]. For example, virally induced expression of ‘yellow cameleon 3.60’ (YC-3.60) in mouse barrel cortex was employed to repeatedly map the location

and spread of whisker-evoked activity in the barrel cortex over several weeks [58] (Fig. 5.1d). Using a transgenic GCaMP3 reporter line [59], large-scale calcium signals were mapped across even larger areas of the somatomotor cortex using a similar approach [60]. Care had to be taken in this study to separate the green calcium indicator fluorescence changes from confounding autofluorescence and intrinsic optical signals. Recently, transgenic mice with widespread GECI expression (e.g., GCaMP6f line, JAX® Mice, Stock Nr. 024107) have been introduced that will be extremely useful for wide-field *in vivo* imaging, in particular when additional specificity is achieved by restricting expression to only particular cortical layers or neuronal subtypes [42].

Cellular Resolution Two-Photon Calcium Imaging

Two-photon excited fluorescence imaging is the key technology that enables high-resolution imaging at substantial depths in cortical tissue [61]. Two-photon calcium imaging is widely used to study neuronal population activity as well as subcellular calcium dynamics in dendrites and dendritic spines in mouse neocortex [48, 62, 63] (Fig. 5.1e and f). Two major paradigm shifts have occurred during the past decade and are still ongoing. First, after an initial phase, in which studies were mainly carried out in anesthetized rats or mice [64–67] the field by now has largely shifted towards imaging in awake, head-restrained animals, following the initial key demonstrations of the feasibility of such experiments [68, 69]. Crucially, cortical imaging in awake animals enables direct observation of neocortical microcircuit dynamics while the brain is in action, best when it is performing a meaningful, task-relevant computation [70] (see below). The second shift seen over the past years is the progressive transition from synthetic calcium indicators to GECIs, fostered by continual improvements of the latter and the advent of sophisticated expression strategies. While bulk-loading with small-molecule indicators continues to be highly suitable for revealing population activity patterns [65, 71, 72], the game-changing advantage of GECIs is the possibility of long-term monitoring of the same neurons and populations over weeks and months [73]. This feature has enabled for instances the investigation of how neuronal activity in mouse barrel cortex reorganizes during sensory deprivation induced by whisker trimming [32] or during learning of a whisker-dependent task [74]. Besides opening the door for such longitudinal studies of changes in network dynamics during plasticity and learning, long-term repeated imaging also turns out helpful in a practical sense for working with well-habituated mice over extended time periods and for making the efforts to train mice in specific behavioral tasks worthwhile.

Local network activity is usually assessed by imaging field-of-views containing tens to several hundred neurons and acquiring time series of two-photon images with frame rates of about 10 Hz for standard and >50 Hz for resonant scanning systems. Free laser scanning techniques for visiting soma after soma can acquire population data with even higher temporal resolution [75, 76]. Irrespective of which laser scanning technique is applied, population calcium imaging in the end provides a multivariate time series data set, containing the time course of action potential-evoked calcium signals for all measured neurons and thus reflecting network dynamics in a high-dimensional state space (with the number of neurons as number

of dimensions). In principle, the neural spike patterns underlying the calcium signals can be estimated from the indicator fluorescence traces using deconvolution techniques [77–80], but much of the analysis can also be carried out on the calcium signals directly. With increasing numbers of neurons being monitored, i.e., sampling network dynamics in even higher-dimensional state space, the demand is now increasing for (semi-)automatized methods for data pre-processing (motion correction, temporal alignment, ROI selection, etc.) and for the application of more sophisticated population analysis tools [81, 82], e.g., for decoding behavioral variables in awake mice [79, 83].

Finally, the high spatial resolution of two-photon microscopy enables *in vivo* imaging of subcellular events, in particular of localized activity in dendrites and at individual synapses (Fig. 5.1f). Thereby, it has become feasible to reveal the spatio-temporal pattern of dendritic activation in the living brain [48], which is essential in order to understand single-neuron computation, i.e., the input-output transformation of a particular cell type. A first goal is to map the spatial distribution of activated synapses by analyzing sensory-evoked subthreshold calcium signals in dendritic spines over substantial portions of the dendritic tree, e.g., following stimulation of different whiskers [84]. Early mapping studies of this sort utilized classical synthetic calcium indicators loaded via whole-cell recording pipettes, but the newest generation of GECIs clearly is capable of resolving single spine activity [50]. Therefore, extended studies of mapping synaptic input patterns, especially during behavior, can be expected for the coming years. A second major goal is to determine in how far and under what conditions the non-linear properties of dendrites become essential. Many neuronal dendrites in principle are capable of producing localized regenerative potentials (‘dendritic spikes’), especially when synaptic inputs are clustered and arrive synchronously. If, how and when this special mode of dendritic integration is relevant is still being worked out in current studies. For example, while most studies agree that NMDA-type glutamate receptors are crucially involved in localized dendritic excitability and calcium signaling, it is still debated under what conditions synaptic integration is rather linear or non-linear, as illustrated by two recent studies on layer 4 neurons in barrel cortex reaching opposite conclusions [85, 86]. Further *in vivo* imaging studies are required to uncover the rules for integration of sensory inputs during specific behavioral conditions in the different neuronal cell types.

Spontaneous Activity and Whisker-Evoked Responses During Anesthesia

Using these various imaging methods, what have we learned about the neocortical representation of whisker movements and touch at the level of cells, local circuits, and cortical hemispheres? Before considering active whisker movements and touch-induced mechanical stimulation, let us first ask what type of spontaneous activity is found in the neocortical network because it is continually active,

whether during sleep, anesthesia, or wakefulness. VSD imaging studies revealed spontaneous waves of activity that travel across cortex, encompassing the barrel field and other areas beyond [36, 37, 87]. During anesthesia, these waves occur at a slow frequency (~ 1 Hz) and correlate well with local field potential (LFP) measurements and with UP and DOWN state membrane potential fluctuations as observed in pyramidal neurons with whole-cell patch pipettes [87]. Interestingly, the spatial dynamics sometimes closely resembles the whisker-evoked activation patterns, an observation that also holds for other sensory modalities and presumably reflects the underlying large-scale functional connectivity across cortical areas [37]. On the cellular level, a consistent finding of electrophysiological and imaging studies is that spontaneous action potential firing rates in layer 2/3 pyramidal neurons are low, typically below 0.5 Hz [66, 88], and that baseline rates increase only slightly ($\sim 30\%$) in awake animals [68]. Juxtacellular recordings from deeper L5 neurons revealed higher baseline firing rates [88], which is hard to compare to optical studies at present because calcium imaging of infragranular layers has remained more challenging (but see [89, 90]).

On all scales, neural responses to whisker stimulation have been measured under anesthesia. Wide-field imaging studies confirm the spatial activation patterns mentioned above, showing an initial activation spot in S1 followed by a second wave of activity emerging from M1 (Fig. 5.2a). Zooming in on the local circuitry in S1 two salient response characteristics have been identified: sparseness and heterogeneity. Layer 2/3 neurons elicit action potentials in response to a whisker stimulus only with a low probability of 0.1–0.4 [66, 67]. Consistently, only a fraction of neurons exhibit suprathreshold responses for a given trial. Moreover, this sparse population activity is quite heterogeneous, it is not normally distributed but displays a skewed, long-tailed distribution with only few percent of strongly responding cells [32]; many neurons show weaker and less reliable responses and a substantial pool mostly remains silent. The functional implications and potential underlying mechanisms of such a sparse and heterogeneous distribution of neuronal network activity are currently being worked out (for review see for example [73, 91, 92]). On the subcellular level, dendritic spine calcium imaging of layer 2 neurons revealed distinct synaptic input patterns when neighboring whiskers of anesthetized mice were stimulated [84]. However, a substantial number of spines were activated by both whiskers, suggesting that these ‘shared inputs’ arrive from neurons that have already integrated the two streams of information.

An important question that so far has been primarily examined under anesthesia is whether feature selectivity maps, analogous to orientation preference maps in visual cortex, exist in the barrel cortex. One possibility is that the cortical responses depend on the direction of whisker deflection (rostral-caudal, ventral-dorsal). Indeed, whisker direction selectivity maps were found inside individual barrel columns using two-photon calcium imaging in rats [93], consistent with earlier electrophysiological work [94]; such maps, however, appeared only in adult animals (with enriched environment) and were not found in young animals [66, 93]. Recently, another type of feature selectivity was described: Population responses of layer 2/3 neurons were examined with two-photon calcium imaging when whiskers were

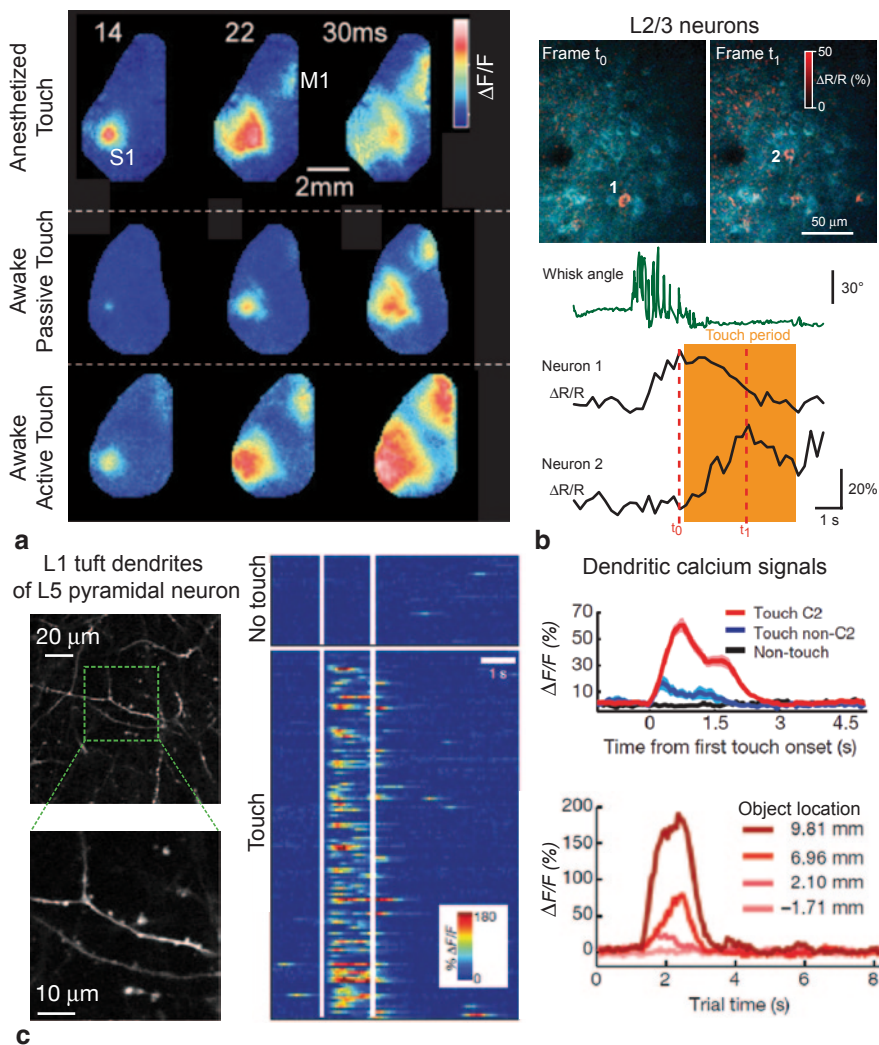


Fig. 5.2 Cortical representations of passive and active whisker touch. **a** Hemisphere-wide cortical activation pattern as revealed with VSD imaging in response to contralateral C2 whisker stimulation (three time points after stimulation shown). A similar pattern of first S1 then M1 activation is seen under three different conditions (3 different mice). (Adapted from Ferezou et al. 2007 [36] with permission). **b** Local circuit activation in layer 2/3 in mouse barrel cortex in response to active texture touch of a sandpaper. $\Delta R/R$ changes of the GECI YC-Nano140 are shown at two time points t_0 and t_1 , just before and during touch. The whiskers are pushed backwards upon contact and the animal stops rhythmic whisking during the touch period. Neuron 1 shows activity correlated with whisking whereas another neuronal subset, including neuron 2, responds during the contact period. (Unpublished data from the Chen et al. 2013b study [80]). **c** Two-photon imaging of distal dendrites of L5 pyramidal neurons in barrel cortex of an awake, head-fixed mouse. The mouse touched with its whiskers a vertical pole presented at different positions as part of an object localization task. *Left*: Zoomed-in two-photon images from L1 dendrites. *Middle*: Dendritic calcium transients with color-coded amplitude in many trials (each row one trial), sorted according to

made to contact textures of different coarseness using artificial whisking [95]. The results suggest that distinct subsets of neurons exhibit preference for different texture coarseness and that these subsets could be organized in spatial clusters and in a columnar fashion. It will be interesting in the future to relate these findings obtained under anesthesia to neuronal response patterns evoked by texture touches in awake animals.

Cortical Representations of Free Whisking and Touch Events in Awake Mice

Several studies have started to apply in vivo imaging methods to investigate cortical activity in the whisker system of awake animals. Most of these studies are now taking advantage of head-fixed paradigms as it turns out that both rats and mice can be well trained to tolerate head fixation [69, 96]. A first question is what activity patterns occur during spontaneous ‘active whisking’ in free air. Calcium imaging of neurons in M1 revealed a relative high fraction of active layer 2/3 neurons, which were classified as ‘whisking neurons’ based on their increased activity during whisking and their ability to decode this behavioral feature [79]; other neurons correlated better with different behavioral features such as object touch or licking. In contrast, using virally induced YC GECIs, we found that the majority of active layer 2/3 neurons in S1 was down-modulated in their activity during free-air whisking but we could also detect a small fraction of neurons (<10%) exhibiting increased activity [97]. Presumably excitatory as well as inhibitory neurons are among these up-modulated neurons but there is also evidence for some cell-type specificity. For example, PV-positive interneurons were always down-modulated, which is consistent with a whole-cell recording study showing reduced firing of fast-spiking interneurons during whisking [22]. Thus, in the supragranular layers of S1 barrel cortex a heterogeneous picture is observed and the same can be expected for other cortical layers and areas. It will be highly informative to employ calcium imaging techniques to determine the sign and strength of modulation for all major cell types throughout S1, M1, and further areas during the simple behavior of voluntary free-air whisking.

During whisker touch events, either ‘passive’ for a quiescent mouse or ‘active’ as induced by whisking, VSD imaging across brain hemispheres has shown a sequential pattern of first S1 and then M1 activation in awake mice similar to the one observed during anesthesia (Fig. 5.2a) [36]. The exact pattern of activation did,

whether a touch occurred or not. *Right top*: Averaged calcium signals aligned to onset of touch for trials with C2 whisker touch (Touch C2), with touch from whiskers other than C2 (Touch non-C2) and with no touch (Non-touch). *Right bottom*: Averaged calcium signals for trials with different object locations. Colors correspond to object locations (measured as the distance of the pole from the centre of the whisker pad along the anterior–posterior axis). (Adapted from Xu et al. 2012 [98] with permission)

however, depend on the behavioral state such that the spread of activity in S1 and particularly the activation of M1 and frontal regions was decreased in trials in which the mouse was either whisking or when the stimulus did not induce a whisking reaction [36]. The tight interplay between S1 and M1 has also been observed in cellular imaging studies. For example, in layer 2/3 of barrel cortex, distinct sparse subsets of neurons are activated upon active touch of a sandpaper, some tightly correlated with the touch period but others correlated with whisking behavior (Fig. 5.2b) [80]. A two-photon imaging study of activity in distal apical tuft dendrites of L5 pyramidal neurons showed a clear correlation of dendritic calcium signals with touch events and interestingly an additional dependency on the object location (Fig. 5.2c) [98]. These studies of neural touch responses in awake mice thus have uncovered functional correlations of the activity in areas, neurons, or dendrites with particular aspects of a touch event. As for free-whisking, it will be essential in the coming years to expand such types of studies to other cortical regions, layers, and cell types in order to obtain a more comprehensive picture of the neural representation of whisker touch in the cortical circuitry. The question remains whether neuronal correlations simply reflect sensory or motor variables or whether neuronal activities are causative for driving behavior. Addressing this issue will be important to fully understand how the neural circuit controlling and processing whisker touches operates. Specific manipulations such as infraorbital nerve transection, localized lesions, or controlled silencing of neural elements using optogenetics and pharmacogenetics will help to dissect causal relationships in the dynamic neural network of the whisker system.

Cortical Dynamics During Tactile Behavioral Tasks

In order to understand sensory processing in the cortex, it is necessary to observe activity patterns under experimental conditions, in which tactile information is used to drive behavior. In order to study how cortical circuits determine behaviorally-relevant parameters such as “where” a stimulus is in the environment and “what” it represents, tasks have been developed for object localization and object discrimination [1]. Since mechanical stability is a fundamental requirement for imaging calcium dynamics in awake animals with standard two-photon microscopes, these tasks have been adopted to head-fixed conditions, which also provide a high degree of stimulus control and behavioral read-out. The mouse is presented with sensory stimuli belonging to two different categories (e.g. anterior vs. posterior position or smooth vs. rough texture). The task of the mouse is to determine the category of a given stimulus and respond with predefined actions such as licking a water port or pressing a lever to obtain reward. During a “go/no-go” task, the animal must initiate an action to obtain a reward following “go” stimuli and withhold the action upon “no-go” stimuli [99]. During a two-alternative forced choice (2AFC) task [100,

101], the animal makes one out of two actions based on the stimuli, e.g., licking one of two water ports positioned to the left or right of the mouth. Each task has its experimental advantages and disadvantages. In the go/no-go task, only the stimuli in “go” trials are potentially rewarding, thus no-go trials can be useful in isolating sensory responses without the potential influence of reward anticipation or response. On the other hand, it can be hard to judge whether no-go trials may also result from a lack of engagement in the task. In 2AFC tasks both categories of stimuli have similar reward predicting values which allows a better readout of reaction time and behavioral state where trials, in which animals fail to respond, can signal lack of motivation or attention. As the animal is supposed to actively respond in each trial, assessment of pure sensory representations may be more difficult, however.

Thus far, object localization during head-fixed tasks has been assessed by presenting a pole along different positions relative to mouse’s head. Population imaging in layer 2/3 of S1 during this task has verified that tactile responses to touch are sparse in this layer with only 10–20% of neurons showing touch-related activity on average [19, 80]. In layer 2/3 of M1, neurons showed correlations with sensory or behavior variables and in well-trained mice neuronal subsets were discriminative for distinguishing trial types such as hits, false alarms, and correct rejections (Fig. 5.3a, b, c) [79]. The sub-cellular resolution of two-photon microscopy provides the unique opportunity to directly observe axonal and dendritic activity during behavior. Activity of long-range inputs can be isolated by imaging spiking-related calcium signals of axons in a region innervated by projection neurons from distant cortical or subcortical areas (Fig. 5.3d, e, f). Calcium imaging of M1 axons innervating S1 has demonstrated that M1 sends information about whisking motor behavior directly to S1 during active tactile sensation [83]. How motor information is integrated into S1 has been studied by complementary work, in which calcium signals were measured in dendritic apical tufts of L5 neurons in S1 [98]. The results suggest that dendrites can non-linearly integrate M1 input carrying information about whisker position with ascending sensory input conveying touch information in order to compute the object position (see Fig. 5.2c).

Object identification has been studied using a texture discrimination task in which mice are trained to report between different panels of sandpaper with different degrees of coarseness (Fig. 5.3g). Calcium imaging of retrogradely labeled S2-projecting and M1-projecting neurons demonstrate that the activity of patterns of these subsets of neurons during texture discrimination differed compared to during object localization (Fig. 5.3h, i). This finding provides a cellular basis for how S1 can support different modes of sensory processing as demanded upon by behavior [80].

It is an open question as to whether the responses observed in sensorimotor cortex during behavior are hardwired within the cortical circuitry or are shaped during learning. Chronic calcium imaging using genetically-encoded calcium indicators provides new opportunities for observing potential changes in cellular responses during perceptual or procedural learning. Initial studies monitoring L2/3 activity in whisker M1 during learning of an object localization task suggest that individual

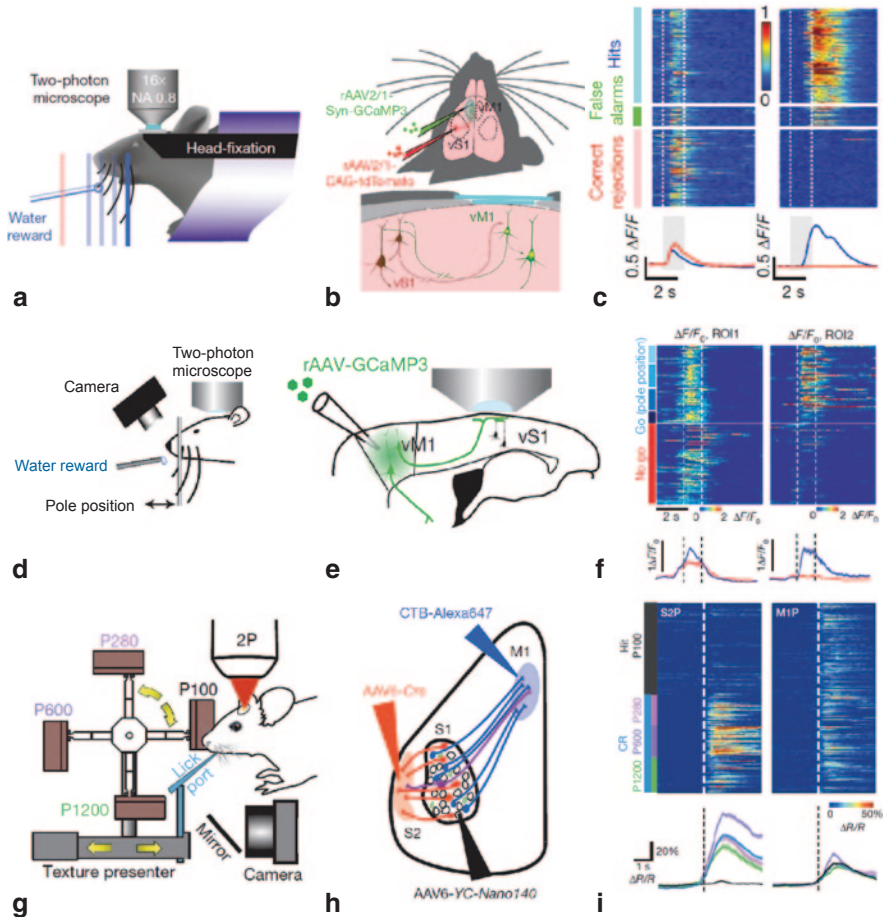


Fig. 5.3 Behavior-related activity of specific elements in cortical circuitry during whisker-based go/no-go tasks. **a** Object detection task. The head-fixed mouse has to detect the presence of a pole presented along the antero-posterior axis. Whisker movements are monitored with a high-speed camera, neuronal population activity in whisker M1 with two-photon calcium imaging. **b** In this study M1 was targeted for GCaMP3 calcium imaging by first injecting a virus causing expression of the red marker tdTomato and then guiding GCaMP3-virus injection by imaging the area of the red axonal projections in M1. **c** Example calcium transients (normalized in amplitude) for two example M1 neurons, sorted according to behavioral outcome. Cell A is active during the whisker sampling period (grey-shaded time period) and shows little trial-type dependence, cell B is active after sensory sampling during licking. (**a-c**) adapted from Huber et al. 2012 [79] with permission. **d** Object localization task in another study, with several go positions and a single no-go pole position in front, similar to (**a**). **e** In this case axonal projections to S1 originating from M1 were made to express GCaMP3 and the terminal axonal arborizations were imaged in S1. **f** Calcium transients for two example ROIs representing two axons, sorted according to trial type (only correct trials shown). While axon 1 shows activity before and during whisking sampling periods, axon 2 is mainly active in trials with strong whisker touches. (**d-f**) adapted from Petreanu et al. 2012 [83] with permission. **g** Texture discrimination task. The mouse has to judge the coarseness of presented sandpapers and lick for a water reward when the target P100 texture is presented. Whisker movements are monitored with a high-speed camera, neuronal population activity in

L2/3 neurons seem to be pre-wired to represent particular motor variables such as whisking or licking through activation of subsets of neurons [79]. However, while population-level representations were stable, the timing and reliability of single neuron responses were dynamic and tracked with motor behavior changes associated with improved task performance. This suggests that a broad repertoire of neuronal responses exist in M1 that is selected for during learning. To what extent S1 responses are shaped in a similar manner during learning remains to be determined.

Conclusions

Looking forward, the imaging methods and molecular techniques developed thus far now presents new opportunities to obtain a comprehensive understanding of vibrissa function in the neocortex during behavior that is integrative along multiple spatial and temporal scales. On the single-neuron level, imaging synaptic activation patterns during behaviors, either by functional measurements of axonal pathways [83, 102] or by direct observation of postsynaptic signals in dendrites with single spine resolution [50], should be highly informative. Such experiments could shed light on the principles of dendritic integration under relevant behavioral conditions. Population imaging of specific neuronal cell types as defined by molecular profile, laminar location, and anatomical connectivity will reveal the functional properties of individual circuit components and their interactions that can be used to determine the computations they perform across different behavioral contexts. Wide-field or large-scale imaging across cortical areas may allow us to better resolve the actual signal flow and understand how local circuit information is exchanged and transformed for sensorimotor integration or feature extraction.

Acknowledgements The authors' work has been supported by the Swiss National Science Foundation (SNSF) (grant 310030-127091 and Sinergia project CRSII3_147660/1; F.H.), a 'Forschungskredit' of the University of Zurich (grant 541541808, J.L.C.) and a fellowship from the U.S. National Science Foundation, International Research Fellowship Program (grant 1158914, J.L.C.).

barrel cortex with two-photon calcium imaging. **h** Labeling strategy to identify projection neurons from S1 to S2 and M1, respectively, using injection of a retrograde infecting AAV6 construct and fluorescently-labeled cholera toxin B subunit (CTB), respectively. In this study the GECI yellow cameleon-Nano140 was applied. **i** Example calcium transients for two neurons in one session, sorted according to behavioral condition. Each row represents the color-coded $\Delta R/R$ change in one trial, aligned to the first moment of touch (dashed line). Average calcium transients are shown at the bottom. Note that the S2-projecting neuron (S2P) is highly discriminative for correct rejection (CR) versus Hit trials, while the M1-projecting neuron (M1P) shows no discriminative power. (**g-i**) adapted from Chen et al. 2013b [80] with permission

References

1. Diamond ME, von Heimendahl M, Knutsen PM, Kleinfeld D, Ahissar E (2008) 'Where' and 'what' in the whisker sensorimotor system. *Nat Rev Neurosci* 9:601–612
2. Petersen CC (2014) Cortical control of whisker movement. *Annu Rev Neurosci* 37:183–203
3. Ahissar E, Kleinfeld D (2003) Closed-loop neuronal computations: focus on vibrissa somatosensation in rat. *Cereb Cortex* 13:53–62
4. Bosman LW, Houweling AR, Owens CB, Tanke N, Shevchouk OT, Rahmati N, Teunissen WH, Ju C, Gong W, Koekkoek SK, De Zeeuw CI (2011) Anatomical pathways involved in generating and sensing rhythmic whisker movements. *Front Integr Neurosci* 5:53
5. Feldman DE (2009) Synaptic mechanisms for plasticity in neocortex. *Annu Rev Neurosci* 32:33–55
6. Feldman DE, Brecht M (2005) Map plasticity in somatosensory cortex. *Science* 310:810–815
7. Margolis DJ, Lütcke H, Helmchen F (2014) Microcircuit dynamics of map plasticity in barrel cortex. *Curr Opin Neurobiol* 24:76–81
8. Aronoff R, Matyas F, Mateo C, Ciron C, Schneider B, Petersen CC (2010) Long-range connectivity of mouse primary somatosensory barrel cortex. *Eur J Neurosci* 31:2221–2233
9. Chakrabarti S, Alloway KD (2006) Differential origin of projections from SI barrel cortex to the whisker representations in SII and M1. *J Comp Neurol* 498(5):624–636
10. Zingg B, Hintiryan H, Gou L, Song MY, Bay M, Bienkowski MS, Foster NN, Yamashita S, Bowman I, Toga AW, Dong HW (2014) Neural networks of the mouse neocortex. *Cell* 156:1096–1111
11. Oh SW, Harris JA, Ng L, Winslow B, Cain N, Mihalas S, Wang QX, Lau C, Kuan L, Henry AM, Mortrud MT, Ouellette B, Nguyen TN, Sorensen SA, Slaughterbeck CR, Wakeman W, Li Y, Feng D, Ho A, Nicholas E, Hirokawa KE, Bohn P, Joines KM, Peng HC, Hawrylycz MJ, Phillips JW, Hohmann JG, Wohnoutka P, Koch C, Bernard A, Dang C, Jones AR, Zeng HK, Gerfen CR (2014) A mesoscale connectome of the mouse brain. *Nature* 508:207
12. Oberlaender M, de Kock CP, Bruno RM, Ramirez A, Meyer HS, Dercksen VJ, Helmstaedter M, Sakmann B (2012) Cell type-specific three-dimensional structure of thalamocortical circuits in a column of rat vibrissal cortex. *Cereb Cortex* 22:2375–2391
13. Meyer HS, Egger R, Guest JM, Foerster R, Reissl S, Oberlaender M (2013) Cellular organization of cortical barrel columns is whisker-specific. *Proc Natl Acad Sci U S A* 110:19113–19118
14. Feldmeyer D (2012) Excitatory neuronal connectivity in the barrel cortex. *Front Neuroanat* 6:24
15. Feldmeyer D, Brecht M, Helmchen F, Petersen CCH, Poulet JFA, Staiger JF, Luhmann HJ, Schwarz C (2013) Barrel cortex function. *Prog Neurobiol* 103:3–27
16. Petersen CC (2007) The functional organization of the barrel cortex. *Neuron* 56:339–355
17. Crochet S, Petersen CC (2006) Correlating whisker behavior with membrane potential in barrel cortex of awake mice. *Nat Neurosci* 9:608–610
18. Petersen CC, Grinvald A, Sakmann B (2003) Spatiotemporal dynamics of sensory responses in layer 2/3 of rat barrel cortex measured in vivo by voltage-sensitive dye imaging combined with whole-cell voltage recordings and neuron reconstructions. *J Neurosci* 23:1298–1309
19. O'Connor DH, Peron SP, Huber D, Svoboda K (2010b) Neural activity in barrel cortex underlying vibrissa-based object localization in mice. *Neuron* 67:1048–1061
20. Sachidhanandam S, Sreenivasan V, Kyriakatos A, Kremer Y, Petersen CCH (2013) Membrane potential correlates of sensory perception in mouse barrel cortex. *Nat Neurosci* 16:1671–1677
21. Gentet LJ (2012) Functional diversity of supragranular GABAergic neurons in the barrel cortex. *Front Neural Circuits* 6:52
22. Gentet LJ, Avermann M, Matyas F, Staiger JF, Petersen CC (2010) Membrane potential dynamics of GABAergic neurons in the barrel cortex of behaving mice. *Neuron* 65:422–435

23. Wang Y, Toledo-Rodriguez M, Gupta A, Wu C, Silberberg G, Luo J, Markram H (2004) Anatomical, physiological and molecular properties of Martinotti cells in the somatosensory cortex of the juvenile rat. *J Physiol* 561:65–90
24. Gentet LJ, Kremer Y, Taniguchi H, Huang ZJ, Staiger JF, Petersen CC (2012) Unique functional properties of somatostatin-expressing GABAergic neurons in mouse barrel cortex. *Nat Neurosci* 15:607–612
25. Rudy B, Fishell G, Lee S, Hjerling-Leffler J (2011) Three groups of interneurons account for nearly 100% of neocortical GABAergic neurons. *Dev Neurobiol* 71:45–61
26. Pi HJ, Hangya B, Kvitsiani D, Sanders JI, Huang ZJ, Kepecs A (2013) Cortical interneurons that specialize in disinhibitory control. *Nature* 503:521
27. Karnani MM, Agetsuma M, Yuste R (2014) A blanket of inhibition: functional inferences from dense inhibitory connectivity. *Curr Opin Neurobiol* 26:96–102
28. Grinvald A, Lieke E, Frostig RD, Gilbert CD, Wiesel TN (1986) Functional architecture of cortex revealed by optical imaging of intrinsic signals. *Nature* 324:361–364
29. Masino SA, Frostig RD (1996) Quantitative long-term imaging of the functional representation of a whisker in rat barrel cortex. *Proc Natl Acad Sci U S A* 93:4942–4947
30. Petersen CCH, Crochet S (2013) Synaptic computation and sensory processing in neocortical layer 2/3. *Neuron* 78:28–48
31. Polley DB, Kvasnak E, Frostig RD (2004) Naturalistic experience transforms sensory maps in the adult cortex of caged animals. *Nature* 429:67–71
32. Margolis DJ, Lütcke H, Schulz K, Haiss F, Weber B, Kügler S, Hasan MT, Helmchen F (2012) Reorganization of cortical population activity imaged throughout long-term sensory deprivation. *Nat Neurosci* 15:1539–1546
33. Arnett MT, Herman DH, McGee AW (2014) Deficits in tactile learning in a mouse model of fragile X syndrome. *PLoS ONE* 9(10):e109116
34. Guy J, Wagener RJ, Mock M, Staiger JF (2014) Persistence of functional sensory maps in the absence of cortical layers in the somatosensory cortex of reeler mice. *Cereb Cortex*. (Epub ahead of print)
35. Grinvald A, Hildesheim R (2004) VSDI: a new era in functional imaging of cortical dynamics. *Nat Rev Neurosci* 5:874–885
36. Ferezou I, Haiss F, Gentet LJ, Aronoff R, Weber B, Petersen CC (2007) Spatiotemporal dynamics of cortical sensorimotor integration in behaving mice. *Neuron* 56:907–923
37. Mohajerani MH, Chan AW, Mohsenvand M, LeDue J, Liu R, McVea DA, Boyd JD, Wang YT, Reimers M, Murphy TH (2013) Spontaneous cortical activity alternates between motifs defined by regional axonal projections. *Nat Neurosci* 16:1426
38. Porter LL, White EL (1983) Afferent and efferent pathways of the vibrissal region of primary motor cortex in the mouse. *J Comp Neurol* 214:279–289
39. Grandy TH, Greenfield SA, Devonshire IM (2012) An evaluation of in vivo voltage-sensitive dyes: pharmacological side effects and signal-to-noise ratios after effective removal of brain-pulsation artifacts. *J Neurophysiol* 108:2931–2945
40. Akemann W, Mutoh H, Perron A, Rossier J, Knöpfel T (2010) Imaging brain electric signals with genetically targeted voltage-sensitive fluorescent proteins. *Nat Methods* 7:643–649
41. Akemann W, Mutoh H, Perron A, Park YK, Iwamoto Y, Knöpfel T (2012) Imaging neural circuit dynamics with a voltage-sensitive fluorescent protein. *J Neurophysiol* 108:2323–2337
42. Madisen L, Garner AR, Shimaoka D, Chuong AS, Klapoetke NC, Li L, van der Bourg A, Niino Y, Egolf L, Monetti C, Gu H, Mills M, Cheng A, Tasic B, Nguyen TN, Sunkin SM, Benucci A, Nagy A, Miyawaki A, Helmchen F, Empson RM, Knöpfel T, Boyden ES, Reid RC, Carandini M, Zeng H (2015) Transgenic mice for intersectional targeting of neural sensors and effectors with high specificity and performance. *Neuron* 85:942–958
43. Kralj JM, Douglass AD, Hochbaum DR, Maclaurin D, Cohen AE (2012) Optical recording of action potentials in mammalian neurons using a microbial rhodopsin. *Nat Methods* 9:90
44. Jin L, Han Z, Platasa J, Wooltorton JRA, Cohen LB, Pieribone VA (2012) Single action potentials and subthreshold electrical events imaged in neurons with a fluorescent protein voltage probe. *Neuron* 75:779–785

45. Gong YY, Wagner MJ, Li JZ, Schnitzer MJ (2014) Imaging neural spiking in brain tissue using FRET-opsin protein voltage sensors. *Nat Commun* 5:3674
46. St-Pierre F, Marshall JD, Yang Y, Gong YY, Schnitzer MJ, Lin MZ (2014) High-fidelity optical reporting of neuronal electrical activity with an ultrafast fluorescent voltage sensor. *Nat Neurosci* 17:884–889
47. Göbel W, Helmchen F (2007a) In vivo calcium imaging of neural network function. *Physiology* 22:358–365
48. Grienberger C, Konnerth A (2012) Imaging calcium in neurons. *Neuron* 73:862–885
49. Miyawaki A, Llopis J, Heim R, McCaffery JM, Adams JA, Ikura M, Tsien RY (1997) Fluorescent indicators for Ca²⁺ based on green fluorescent proteins and calmodulin. *Nature* 388:882–887
50. Chen TW, Wardill TJ, Sun Y, Pulver SR, Renninger SL, Baohan A, Schreiter ER, Kerr RA, Orger MB, Jayaraman V, Looger LL, Svoboda K, Kim DS (2013c) Ultrasensitive fluorescent proteins for imaging neuronal activity. *Nature* 499:295–300
51. Ohkura M, Sasaki T, Sadakari J, Gengyo-Ando K, Kagawa-Nagamura Y, Kobayashi C, Ikegaya Y, Nakai J (2012) Genetically encoded green fluorescent Ca²⁺ indicators with improved detectability for neuronal Ca²⁺ signals. *PLoS ONE* 7:e51286
52. Nagai T, Yamada S, Tominaga T, Ichikawa M, Miyawaki A (2004) Expanded dynamic range of fluorescent indicators for Ca²⁺ by circularly permuted yellow fluorescent proteins. *Proc Natl Acad Sci U S A* 101:10554–10559
53. Horikawa K, Yamada Y, Matsuda T, Kobayashi K, Hashimoto M, Matsu-ura T, Miyawaki A, Michikawa T, Mikoshiba K, Nagai T (2010) Spontaneous network activity visualized by ultrasensitive Ca²⁺ indicators, yellow Cameleon-Nano. *Nat Methods* 7:729–732
54. Mank M, Santos AF, Drenth S, Mrcic-Flogel TD, Hofer SB, Stein V, Hendel T, Reiff DF, Levelt C, Borst A, Bonhoeffer T, Hubener M, Griesbeck O (2008) A genetically encoded calcium indicator for chronic in vivo two-photon imaging. *Nat Methods* 5:805–811
55. Thestrup T, Litzlbauer J, Bartholomaeus I, Mues M, Russo L, Dana H, Kovalchuk Y, Liang YJ, Kalamakis G, Laukat Y, Becker S, Witte G, Geiger A, Allen T, Rome LC, Chen TW, Kim DS, Garaschuk O, Griesinger C, Griesbeck O (2014) Optimized ratiometric calcium sensors for functional in vivo imaging of neurons and T lymphocytes. *Nat Methods* 11:175
56. Berger T, Borgdorff A, Crochet S, Neubauer FB, Lefort S, Fauvet B, Ferezou I, Carleton A, Lüscher HR, Petersen CCH (2007) Combined voltage and calcium epifluorescence imaging in vitro and in vivo reveals subthreshold and suprathreshold dynamics of mouse barrel cortex. *J Neurophysiol* 97:3751–3762
57. Lütcke H, Murayama M, Hahn T, Margolis DJ, Astori S, Zum Alten Borgloh SM, Göbel W, Yang Y, Tang W, Kügler S, Sprengel R, Nagai T, Miyawaki A, Larkum ME, Helmchen F, Hasan MT (2010) Optical recording of neuronal activity with a genetically-encoded calcium indicator in anesthetized and freely moving mice. *Front Neural Circuits* 4:9
58. Minderer M, Liu W, Sumanovski LT, Kügler S, Helmchen F, Margolis DJ (2012) Chronic imaging of cortical sensory map dynamics using a genetically encoded calcium indicator. *J Physiol* 590:99–107
59. Zariwala HA, Borghuis BG, Hoogland TM, Madisen L, Tian L, De Zeeuw CI, Zeng H, Looger LL, Svoboda K, Chen TW (2012) A Cre-dependent GCaMP3 reporter mouse for neuronal imaging in vivo. *J Neurosci* 32:3131–3141
60. Vanni MP, Murphy TH (2014) Mesoscale transcranial spontaneous activity mapping in GCaMP3 transgenic mice reveals extensive reciprocal connections between areas of somatomotor cortex. *J Neurosci* 34:15931–15946
61. Helmchen F, Denk W (2005) Deep tissue two-photon microscopy. *Nat Methods* 2:932–940
62. Grewe BF, Helmchen F (2009) Optical probing of neuronal ensemble activity. *Curr Opin Neurobiol* 19:520–529
63. Lütcke H, Helmchen F (2011) Two-photon imaging and analysis of neural network dynamics. *Rep Prog Phys* 74(8):086602
64. Ohki K, Chung S, Ch'ng Y, Kara P, Reid R (2005) Functional imaging with cellular resolution reveals precise micro-architecture in visual cortex. *Nature* 433:597–603

65. Kerr JND, Greenberg D, Helmchen F (2005) Imaging input and output of neocortical networks in vivo. *Proc Natl Acad Sci U S A* 102:14063–14068
66. Kerr JN, de Kock CP, Greenberg DS, Bruno RM, Sakmann B, Helmchen F (2007) Spatial organization of neuronal population responses in layer 2/3 of rat barrel cortex. *J Neurosci* 27:13316–13328
67. Sato TR, Gray NW, Mainen ZF, Svoboda K (2007) The functional microarchitecture of the mouse barrel cortex. *PLoS Biol* 5:e189
68. Greenberg DS, Houweling AR, Kerr JN (2008) Population imaging of ongoing neuronal activity in the visual cortex of awake rats. *Nature Neurosci* 11(7):749–751
69. Dombeck DA, Khabbaz AN, Collman F, Adelman TL, Tank DW (2007) Imaging large-scale neural activity with cellular resolution in awake, mobile mice. *Neuron* 56:43–57
70. Chen JL, Andermann ML, Keck T, Xu NL, Ziv Y (2013a) Imaging neuronal populations in behaving rodents: paradigms for studying neural circuits underlying behavior in the mammalian cortex. *J Neurosci* 33:17631–17640
71. Stosiek C, Garaschuk O, Holthoff K, Konnerth A (2003) In vivo two-photon calcium imaging of neuronal networks. *Proc Natl Acad Sci USA* 100:7319–7324
72. Dombeck DA, Graziano MS, Tank DW (2009) Functional clustering of neurons in motor cortex determined by cellular resolution imaging in awake behaving mice. *J Neurosci* 29:13751–13760
73. Lütcke H, Margolis DJ, Helmchen F (2013b) Steady or changing? Long-term monitoring of neuronal population activity. *Trends Neurosci* 36:375–384
74. Chen JL, Margolis DJ, Stankov A, Sumanovski LT, Schneider BL, Helmchen F (2015) Pathway-specific reorganization of projection neurons in somatosensory cortex during learning. *Nat Neurosci* 2015 Jun 22, (Epub ahead of print)
75. Göbel W, Helmchen F (2007b) New angles on neuronal dendrites in vivo. *J Neurophysiol* 98:3770–3779
76. Lillis KP, Eng A, White JA, Mertz J (2008) Two-photon imaging of spatially extended neuronal network dynamics with high temporal resolution. *J Neurosci Methods* 172:178–184
77. Vogelstein JT, Packer AM, Machado TA, Sippy T, Babadi B, Yuste R, Paninski L (2010) Fast nonnegative deconvolution for spike train inference from population calcium imaging. *J Neurophysiol* 104:3691–3704
78. Lütcke H, Gerhard F, Zenke F, Gerstner W, Helmchen F (2013a) Inference of neuronal network spike dynamics and topology from calcium imaging data. *Front Neural Circuits* 7:201
79. Huber D, Gutnisky DA, Peron S, O'Connor DH, Wiegert JS, Tian L, Oertner TG, Looger LL, Svoboda K (2012) Multiple dynamic representations in the motor cortex during sensorimotor learning. *Nature* 484:473–478
80. Chen JL, Carta S, Soldado-Magraner J, Schneider BL, Helmchen F (2013b) Behaviour-dependent recruitment of long-range projection neurons in somatosensory cortex. *Nature* 499:336–340
81. Mukamel EA, Nimmerjahn A, Schnitzer MJ (2009) Automated analysis of cellular signals from large-scale calcium imaging data. *Neuron* 63:747–760
82. Freeman J, Vladimirov N, Kawashima T, Mu Y, Sofroniew NJ, Bennett DV, Rosen J, Yang CT, Looger LL, Ahrens MB (2014) Mapping brain activity at scale with cluster computing. *Nat Methods* 11:941–950
83. Petreanu L, Gutnisky DA, Huber D, Xu NL, O'Connor DH, Tian L, Looger L, Svoboda K (2012) Activity in motor-sensory projections reveals distributed coding in somatosensation. *Nature* 489:299–303
84. Varga Z, Jia HB, Sakmann B, Konnerth A (2011) Dendritic coding of multiple sensory inputs in single cortical neurons in vivo. *Proc Natl Acad Sci U S A* 108:15420–15425
85. Lavzin M, Rapoport S, Polsky A, Garion L, Schiller J (2012) Nonlinear dendritic processing determines angular tuning of barrel cortex neurons in vivo. *Nature* 490:397–401
86. Jia HB, Varga Z, Sakmann B, Konnerth A (2014) Linear integration of spine Ca²⁺ signals in layer 4 cortical neurons in vivo. *Proc Natl Acad Sci U S A* 111:9277–9282
87. Ferezou I, Bolea S, Petersen CC (2006) Visualizing the cortical representation of whisker touch: voltage-sensitive dye imaging in freely moving mice. *Neuron* 50:617–629

88. de Kock CP, Sakmann B (2009) Spiking in primary somatosensory cortex during natural whisking in awake head-restrained rats is cell-type specific. *Proc Natl Acad Sci U S A* 106:16446–16450
89. Mittmann W, Wallace DJ, Czubayko U, Herb JT, Schaefer AT, Looger LL, Denk W, Kerr JN (2011) Two-photon calcium imaging of evoked activity from L5 somatosensory neurons in vivo. *Nat Neurosci* 14:1089–1093
90. Andermann ML, Gilfof NB, Goldey GJ, Sachdev RN, Wolfel M, McCormick DA, Reid RC, Levene MJ (2013) Chronic cellular imaging of entire cortical columns in awake mice using microprisms. *Neuron* 80:900–913
91. Barth AL, Poulet JFA (2012) Experimental evidence for sparse firing in the neocortex. *Trends Neurosci* 35:345–355
92. Buzsaki G, Mizuseki K (2014) The log-dynamic brain: how skewed distributions affect network operations. *Nat Rev Neurosci* 15:264–278
93. Kremer Y, Leger JF, Goodman D, Brette R, Bourdieu L (2011) Late emergence of the vibrissa direction selectivity map in the rat barrel cortex. *J Neurosci* 31:14831–14831
94. Andermann ML, Moore CI (2006) A somatotopic map of vibrissa motion direction within a barrel column. *Nat Neurosci* 9:543–551
95. Garion L, Dubin U, Rubin Y, Khateb M, Schiller Y, Azouz R, Schiller J (2014) Texture coarseness responsive neurons and their mapping in layer 2–3 of the rat barrel cortex in vivo. *Elife* 3:e03405
96. Schwarz C, Hentschke H, Butovas S, Haiss F, Stuttgen MC, Gerdjikov TV, Bergner CG, Waiblinger C (2010) The head-fixed behaving rat—procedures and pitfalls. *Somatosens Mot Res* 27:131–148
97. Schulz K, Schrepfer I, Margolis DJ, Lütcke H, Kügler S, Hasan MT, Helmchen F (2010) Whisking-induced modulation of L2/3 population activity imaged in awake head-fixed mice. Society of Neuroscience abstract. Program No 58718, 2010, Neuroscience Meeting Planner, San Diego, CA
98. Xu NL, Harnett MT, Williams SR, Huber D, O'Connor DH, Svoboda K, Magee JC (2012) Nonlinear dendritic integration of sensory and motor input during an active sensing task. *Nature* 492:247–251
99. O'Connor DH, Clack NG, Huber D, Komiyama T, Myers EW, Svoboda K (2010a) Vibrissa-based object localization in head-fixed mice. *J Neurosci* 30:1947–1967
100. Mayrhofer JM, Skreb V, von der Behrens W, Musall S, Weber B, Haiss F (2013) Novel two-alternative forced choice paradigm for bilateral vibrotactile whisker frequency discrimination in head-fixed mice and rats. *J Neurophysiol* 109:273–284
101. O'Connor DH, Hires SA, Guo ZV, Li N, Yu J, Sun QQ, Huber D, Svoboda K (2013) Neural coding during active somatosensation revealed using illusory touch. *Nat Neurosci* 16:958–965
102. Glickfeld LL, Andermann ML, Bonin V, Reid RC (2013) Cortico-cortical projections in mouse visual cortex are functionally target specific. *Nat Neurosci* 16:219–226